Iranian Journal of Numerical Analysis and Optimization
Vol. ??, No. ??, ??, pp ??
https://doi.org/??
https://ijnao.um.ac.ir/

Research Article

The analysis of the mathematical stability of a cholera disease model

I. Sahib*, M. Baroudi, H. Gourram, B. Khajji, A. Labzai and M. Belam

*Corresponding author

Received ??? ; revised ??? ; accepted ???

Issam Sahib
Laboratory LMACS, Sultan Moulay Slimane University, MATIC Research Team: Applied Mathematics and Information and Communication Technologie, Department of Mathematics and Computer Science, Khouribga Polydisciplinary Faculty, Morocco.. e-mail: sahibissam@gmail.com

Mohamed Baroudi
Laboratory LMACS, Sultan Moulay Slimane University, MATIC Research Team: Applied Mathematics and Information and Communication Technologie, Department of Mathematics and Computer Science, Khouribga Polydisciplinary Faculty, Morocco. e-mail: m.mohamed.baroudi@gmail.com

Hicham Gourram
Laboratory LMACS, Sultan Moulay Slimane University, MATIC Research Team: Applied Mathematics and Information and Communication Technologie, Department of Mathematics and Computer Science, Khouribga Polydisciplinary Faculty, Morocco. e-mail: gourramhicham03@gmail.com

Bouchaib Khajji
Laboratory of Analysis Modeling and Simulation, Department of Mathematics and Computer Science, Faculty of Sciences Ben M'sik, Hassan II University of Casablanca, Morocco. e-mail: labzaiabdo1977@gmail.com

Abderrahim Labzai
Laboratory of Analysis Modeling and Simulation, Department of Mathematics and Computer Science, Faculty of Sciences Ben M'sik, Hassan II University of Casablanca, Mo-

Abstract

In this study, we develop a deterministic model for cholera transmission dynamics, incorporating vaccination campaigns, treatment of infected individuals, and water sanitation initiatives. A novel feature of our model is the inclusion of healthcare centers, which enhances the simulation of treatment dynamics, offering new insights into cholera management. The model's central metric is the basic reproduction number R_0, derived from the disease-free equilibrium (DFE) condition. Stability analysis shows that when $R_0 \leq 1$, the DFE is asymptotically stable, ensuring cholera eradication, while $R_0 > 1$ leads to an endemic equilibrium. Sensitivity analysis highlights that vaccination, treatment, sanitation, and public awareness campaigns are critical for reducing R_0. The inclusion of healthcare centers further improves the model's effectiveness by ensuring timely treatment. Numerical simulations, validated using $MATLAB$, confirm that comprehensive public health strategies, including expanded vaccination campaigns and healthcare infrastructure, are essential for combating cholera outbreaks. This model underscores the importance of timely medical intervention in reducing infection rates and fatalities.

AMS subject classifications (2020): 49J15, 93C10, 92B05, 93A30.

Keywords: stability; sensitivity; optimal control; Disease cholera.

1 Introduction

Cholera remains a significant global public health threat, responsible for tens of thousands of deaths each year [22]. This highly contagious disease, caused

rocco. e-mail: khajjibouchaib@gmail.com

Mohamed Belam
Laboratory LMACS, Sultan Moulay Slimane University, MATIC Research Team: Applied Mathematics and Information and Communication Technologie, Department of Mathematics and Computer Science, Khouribga Polydisciplinary Faculty, Morocco. e-mail: m.belam@gmail.com

How to cite this article
Sahib, I., Baroudi, M., Gourram, H., Khajji, B., Labzai, A. and Belam, M., The analysis of the mathematical stability of a cholera disease model. *Iran. J. Numer. Anal. Optim.*, ??; ??(??): ??-??. ??

by the bacterium *Vibrio cholerae*, spreads rapidly in communities through contaminated water and food sources. The transmission dynamics of cholera within a community are influenced by a complex interaction of social, environmental, and behavioral factors. In certain regions, the periodic recurrence of cholera outbreaks can be attributed in part to seasonal variations in contact rates, water quality, and sanitation levels [6, 15]. Understanding and accurately estimating the prevalence of *Vibrio cholerae* infections in endemic populations, as well as the correlation between the concentration of the bacteria and its virulence, is crucial to controlling the spread of the disease and mitigating its impact [3]. These seasonal fluctuations are particularly important in explaining the cyclical nature of cholera outbreaks [8].

Mathematical models have played a crucial role in capturing these dynamics. In 2001, scientists enhanced Capasso's model by incorporating the environmental component, specifically the concentration of *Vibrio cholerae* in the water supply, into a basic SIR (Susceptible-Infected-Recovered) model. This modification allowed for a better understanding of how the presence of the bacteria in water sources contributes to the incidence of cholera. The saturation effect of bacterial concentration was modeled using a logistic function, reflecting the nonlinear relationship between bacterial load and infection risk.

Further advancements in modeling cholera transmission were made by Hartley [10], who introduced a hyper-infectious stage for *Vibrio cholerae*. This addition, based on observations from laboratory settings, captured the highly transmissible nature of recently shed *Vibrio cholerae*, which is particularly potent immediately after being excreted by infected individuals [8]. This feature significantly enhances the pathogen's ability to spread during an outbreak, emphasizing the need for rapid and targeted interventions to control the transmission of this highly contagious form. Hartley's work underscored the importance of considering pathogen dynamics when designing intervention strategies. It is imperative to explore whether other common infectious diseases also exhibit such hyper-transmissible stages and, if so, to incorporate these stages into their respective prevention models to ensure a more comprehensive and effective response.

Nelson et al. [17] further refined these models by incorporating a more accurate representation of the pathogen's infectious dose, recognizing that the minimal dose required to cause an infection plays a critical role in determining how quickly an outbreak can spread. Interventions that focus on reducing exposure to the hyper-infectious form of *Vibrio cholerae*, such as improved sanitation and clean water distribution, are essential for preventing large-scale outbreaks. Moreover, evaluating other diseases for similar hyper-infectious conditions and integrating such findings into disease prevention models will allow for more targeted and efficient public health interventions [19].

Raising public awareness through campaigns and educational initiatives has proven to be an effective strategy for controlling the spread of infectious diseases. By reducing the likelihood of contact transmission among vulnerable populations, awareness campaigns play a pivotal role in managing epidemics. In the digital age, the rapid dissemination of information through social media, coupled with increased global travel, has made awareness even more critical. These campaigns can significantly decrease the probability of transmission by educating the public on hygiene practices and the importance of early detection and treatment, ultimately improving the overall dynamics of epidemics [1, 16, 25].

The relationship between the spread of infectious diseases and human social behavior has been extensively studied in both theoretical and empirical research. Numerous mathematical models have been developed to explore these interactions, particularly in the context of cholera [4, 5, 9, 11, 13, 16, 20]. These models have helped public health officials design strategies to reduce the number of cholera cases and improve overall health outcomes in affected communities [18].

In this study, we delve deeply into the foundational mathematical components of cholera models, focusing on critical aspects such as the determination of equilibrium points and the calculation of the epidemic threshold, commonly referred to as the basic reproductive number R_0. The stability of these equilibrium points is rigorously analyzed, revealing the conditions under which the disease-free equilibrium (DFE) is globally asymptotically stable (GAS). Descartes' rule of signs is applied to derive global stability conditions, and

the local stability of the endemic equilibrium is evaluated using the center manifold theory [15]. These analyses provide valuable insights into the underlying dynamics of cholera transmission and the potential for controlling outbreaks through targeted interventions.

One critical aspect that has not been fully explored in many models is the role of healthcare infrastructure in managing cholera outbreaks. Integrating healthcare centers into the model is essential for accurately capturing the real-world dynamics of disease transmission and control. Healthcare centers are often the first line of defense during an outbreak, providing immediate treatment to those infected and acting as central points for public health interventions such as vaccination, water sanitation programs, and public awareness campaigns. By incorporating healthcare facilities into the model, we can simulate more realistic outbreak scenarios and assess the impact of different intervention strategies in a variety of contexts.

The inclusion of healthcare centers also allows for the optimization of resource allocation during an outbreak. For instance, the model can help determine the most efficient distribution of medical supplies and personnel across different regions, ensuring that healthcare resources are concentrated in areas where they will have the greatest impact. This addition not only enhances the accuracy and realism of the model but also provides public health officials with a powerful tool for decision-making in the midst of an outbreak. The importance of this integration cannot be overstated, as it bridges the gap between theoretical models and practical applications in public health policy.

In conclusion, this study builds upon existing cholera models by not only refining the mathematical understanding of cholera dynamics but also by emphasizing the critical role of healthcare infrastructure in controlling outbreaks. By combining rigorous mathematical analysis with practical considerations of public health intervention, this model provides a more comprehensive and applicable tool for managing cholera outbreaks and potentially other infectious diseases as well.

The paper is organized as follows: A mathematical model and its basic properties are presented in Section 2. The features of the model's local and global asymptotic stability are examined in Section 3. The sensitivity of the basic reproduction number concerning the model parameters is investigated

in Section 4. Numerical simulations and discussions are provided in Section 5. The paper is finally concluded in Section 6.

2 Fundamental properties and the mathematical model

2.1 A mathematical model

In the context of cholera, we introduce a continuous dynamics model of the SICR-B (Susceptible-Infectious-Centers-Recovered-Bacterial) type, which includes a category for bacterial concentration. The total population, $N(t)$, is divided into four classes: susceptible individuals $S(t)$, infected individuals $I(t)$ exhibiting symptoms, individuals undergoing treatment in centers $C(t)$, and recovered individuals $R(t)$. The total population at time t is given by $N(t) = S(t) + I(t) + C(t) + R(t)$. The graphical representation of this model is shown in Figure 1.

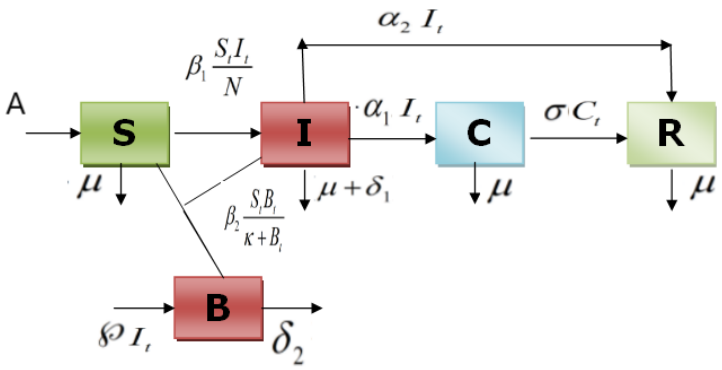

Figure 1: The dynamics among the five compartments SICR-B of cholera disease.

We study five nonlinear differential equations:

$$\begin{cases} \dfrac{dS(t)}{dt} = \mathrm{A} - \mu S - \beta_1 \dfrac{SI}{N} - \beta_2 \dfrac{SB}{\kappa + B}, \\ \dfrac{dI(t)}{dt} = \beta_1 \dfrac{SI}{N} - I(\mu + \delta_1 + \alpha_1 + \alpha_2) + \beta_2 \dfrac{SB}{\kappa + B}, \\ \dfrac{dC(t)}{dt} = \alpha_1 I - (\sigma + \mu)C, \\ \dfrac{dR(t)}{dt} = \alpha_2 I + \sigma C - \mu R, \\ \dfrac{dB(t)}{dt} = \wp I - \delta_2 B. \end{cases} \tag{1}$$

The initial states are given as $S(0) \geq 0$, $I(0) \geq 0$, $C(0) \geq 0$, $R(0) \geq 0$, and $B(0) \geq 0$. The total population $N(t)$ at time $t > 0$ is categorized into four classes: Susceptible individuals $S(t)$, infectious individuals $I(t)$ showing symptoms, individuals undergoing treatment in centers $C(t)$, and recovered individuals $R(t)$.

Additionally, we introduce a class $B(t)$ representing bacterial concentration at time t. We assume a positive recruitment rate A into the susceptible class $S(t)$ and a positive natural death rate μ for all time t. Susceptible individuals can contract cholera at a rate $\beta_2 \frac{B(t)}{\kappa + B(t)}$, where $\beta_2 > 0$ is the ingestion rate of bacteria from contaminated sources, κ is the half-saturation constant of the bacteria population, and $\frac{B(t)}{\kappa + B(t)}$ represents the probability of infection given exposure.

Infected individuals can opt for treatment in centers for a period, where they are isolated and receive appropriate medication at rates α_1 and α_2. Recovery from treatment occurs at rate σ. Disease-related death rates for infected individuals undergoing treatment and those not in treatment are δ_1 and μ, respectively.

Each infected individual contributes to an increase in bacterial concentration at rate $\wp$, while the bacterial concentration decreases due to mortality at rate δ_2.

2.2 Fundamental characteristics of the model

2.2.1 Region of invariance

It is necessary to demonstrate that all solutions of system (1) starting from positive initial values will remain positive for all $t > 0$. This will be established through the following lemma.

Lemma 1. All admissible solutions $S(t), I(t), C(t), R(t)$, and $B(t)$ of system (1) are bounded within the region $\Omega = \Omega_N * \Omega_B$, where

$$\begin{cases} \Omega_N = \left\{ (S, I, C, R) \in \mathbb{R}^4_+ : S + I + C + R \leq \frac{\mathrm{A}}{\mu} \right\}, \\ \Omega_B = \left\{ B \in \mathbb{R}_+ : B \leq \frac{\wp}{\delta_2} \right\}. \end{cases} \tag{2}$$

Proof. From the equation of system (1)

$$\frac{dN(t)}{dt} = \mathrm{A} - \mu N(t) - I\delta_1, \tag{3}$$

implies the following equation:

$$\frac{dN(t)}{dt} \leq \mathrm{A} - \mu N(t). \tag{4}$$

Therefore, it is clear that

$$N(t) \leq \frac{\mathrm{A}}{\mu}(1 - e^{-\mu t}) + N(0)e^{-\mu t}. \tag{5}$$

Since $N(0)$ is the initial value of the total number of people,

$$\lim_{t \to +\infty} SupN(t) \leq \frac{\mathrm{A}}{\mu}. \tag{6}$$

Then

$$S(t) + I(t) + C(t) + R(t) \leq \frac{\mathrm{A}}{\mu}. \tag{7}$$

Similarly,

$$\frac{dB(t)}{dt} = \wp I - \delta_2 B(t) \leq \wp - \delta_2 B(t), \tag{8}$$

$$B(t) \leq \frac{\wp}{\delta_2} + B(0)e^{-\delta_2 t}, \tag{9}$$

$$\lim_{t \to +\infty} SupB(t) \leq \frac{\wp}{\delta_2}, \tag{10}$$

$$[B(t) \leq \frac{\wp}{\delta_2}. \tag{11}$$

For the analysis of model (1), we get the regions, which is given by the set $\Omega = \Omega_N * \Omega_B$, where

$$\begin{cases} \Omega_N = \left\{(S, I, C, R) \in \mathbb{R}^4_+ : S + I + C + R \leq \frac{\mathrm{A}}{\mu}\right\}, \\ \Omega_B = \left\{B \in \mathbb{R}_+ : B \leq \frac{\wp}{\delta_2}\right\}, \end{cases} \tag{12}$$

which is a positively invariant set for (1). Therefore, it is only necessary to consider the dynamics of the system (1) in relation to the set of nonnegative solutions Ω. □

2.2.2 Positivity of the model's solutions.

Theorem 1. If $S(0) \geq 0$, $I(0) \geq 0$, $C(0) \geq 0$, $R(0) \geq 0$, and $B(0) \geq 0$, then the solutions of system equation (1), $S(t), I(t), C(t), R(t)$, and $B(t)$ are positive for all $t > 0$.

Proof. Starting from the first equation of system (1), we obtain

$$\frac{dS(t)}{dt} = \mathrm{A} - M(t)S(t). \tag{13}$$

Given that

$$M(t) = \mu + \beta_1 \frac{I(t)}{N} + \beta_2 \frac{B(t)}{\kappa + B(t)}, \tag{14}$$

We multiply (13) by $\exp\left(\int_0^t M(s)\, ds\right)$; then we obtain

$$\frac{dS(t)}{dt} * \exp(\int_0^t M(s)ds) = [\mathrm{A} - M(t) * S(t)] * \exp(\int_0^t M(s)ds), \tag{15}$$

$$\frac{dS(t)}{dt} * \exp(\int_0^t M(s)ds) + M(t) * S(t) * \exp(\int_0^t M(s)ds) = \mathrm{A} * \exp(\int_0^t M(s)ds). \tag{16}$$

Therefore

$$\frac{d}{dt}[S(t) * \exp(\int_0^t M(s)ds] = \mathrm{A} * \exp(\int_0^t M(s)ds). \tag{17}$$

When we take the integral with respect to s from 0 to t, we obtain

$$S(t) * \exp(\int_0^t M(s)ds) - S(0) = \mathrm{A} * \int_0^t (\exp(\int_0^w M(s)ds))dw. \tag{18}$$

Multiplying (18) by $\exp\left(-\int_0^t M(s)\,ds\right)$, we obtain

$$\begin{aligned} &S(t) - S(0) * \exp(-\int_0^t M(s)ds) \\ &= \mathrm{A} * \exp(-\int_0^t M(s)ds) * \int_0^t (\exp(\int_0^w M(s)ds))dw. \end{aligned} \tag{19}$$

Then

$$\begin{aligned} S(t) =& S(0) * \exp(-\int_0^t M(s)ds) \\ &+ \mathrm{A} * \exp(-\int_0^t M(s)ds) * \int_0^t (\exp(\int_0^w M(s)ds))dw \geq 0. \end{aligned}$$

Thus, $S(t)$ is a positive solution. Similarly, based on the other equations in system (1), we obtain

$$I(t) \geq I(0) * \exp(-\int (\mu + \delta_1 + \alpha_1 + \alpha_2 - \beta_1 \frac{S(s)}{N})ds \geq 0, \tag{20}$$

$$\begin{cases} C(t) \geq C(0).\exp(-(\sigma + \mu)t) \geq 0, \\ R(t) \geq R(0).\exp(-(\alpha_2 + \mu)t) \geq 0, \\ B(t) \geq B(0).\exp(-\delta_2 t) \geq 0. \end{cases} \tag{21}$$

As a result, the proof is finished since we can see that for all $t \geq 0$, the solutions $S(t)$, $I(t)$, $C(t)$, $R(t)$, and $B(t)$ to the system (1) are positive. Since the variables C and R do not affect the first three equations in system (1), the dynamics of equation system (1) is equal to the dynamics of equation system:

$$\begin{cases} \frac{dS(t)}{dt} = \mathrm{A} - \mu S - \beta_1 \frac{SI}{N} - \beta_2 \frac{SB}{\kappa + B}, \\ \frac{dI(t)}{dt} = \beta_1 \frac{SI}{N} - I(\mu + \delta_1 + \alpha_1 + \alpha_2) + \beta_2 \frac{SB}{\kappa + B}, \\ \frac{dB(t)}{dt} \wp I - \delta_2 B. \end{cases} \tag{22}$$

□

2.3 An examination of the model's sensitivity and stability.

2.3.1 Points of equilibrium:

There are two equilibrium points in this model: The DFE point, which occurs when cholera is absent, and the epidemic equilibrium point, which occurs when cholera is present. By setting the derivatives of the rate of change expressions in the (22) system to zero, these points can be determined.

In the absence of a virus ($I = B = 0$), the Cholera DFE $E^0_{eq} = (\frac{A}{\mu}, 0, 0)$ is reached. When the disease exists ($I \neq 0$ *and* $B \neq 0$), the present equilibrium of the Cholera disease is reached, denoted by $E^*_{eq} = (S^*; E^*; I^*)$. To calculate the fundamental reproduction number R_0, we will apply the next-generation operator method.

R_0 is the basic reproduction number.

Diekmann et al. [2] defined the basic reproduction number (R_0), which is an important indicator of the transmissibility of an infectious disease in epidemiology. In a population that is fully susceptible, it denotes the average number of secondary infections caused by one infected person. The mathematical method R_0 is computed using the next-generation matrix approach [21].

The spectral radius of the product matrix FV^{-1} is denoted by the basic reproduction number R_0. In other words, $R_0 = \rho(FV^{-1})$, where the spectral radius is indicated by ρ.

We define F as a nonnegative matrix accounting for the new infective terms within the next-generation matrix approach framework. Comparably, both of the remaining transfer terms are represented by V, which is a non-singular M-matrix evaluated at the DFE. Then

$$F = \begin{pmatrix} \beta_1 \dfrac{\mathrm{A}}{\mu N} & \beta_2 \dfrac{\mathrm{A}}{\kappa\mu} \\ 0 & 0 \end{pmatrix}, \tag{23}$$

$$V = \begin{pmatrix} (\mu + \delta_1) + (\alpha_1 + \alpha_2) & 0 \\ -\wp & \delta_2 \end{pmatrix}, \tag{24}$$

$$V^{-1} = \begin{pmatrix} \frac{1}{(\mu+\delta_1)+(\alpha_1+\alpha_2)} & 0 \\ \frac{\wp}{\delta_2[(\mu+\delta_1)+(\alpha_1+\alpha_2)]} & \frac{1}{\delta_2} \end{pmatrix}, \tag{25}$$

$$F.V^{-1} \tag{26}$$
$$= \begin{pmatrix} \beta_1 \frac{\mathrm{A}}{\mu N[(\mu+\delta_1)+(\alpha_1+\alpha_2)]} + \beta_2 \frac{\mathrm{A}\wp}{\delta_2\kappa\mu[(\mu+\delta_1)+(\alpha_1+\alpha_2)]} & \beta_2 \frac{\mathrm{A}}{\kappa\mu\delta_2} \\ 0 & 0 \end{pmatrix}.$$

This suggests that R_0, the basic reproduction number, can be found by using the following relationships (where ρ is the spectral radius):

$$R_0 = \rho(F.V^{-1}), \tag{27}$$

$$R_0 = \beta_1 \frac{\mathrm{A}}{\mu N(\mu+\delta_1+\alpha_1+\alpha_2)} + \beta_2 \frac{\mathrm{A}\wp}{\delta_2\kappa\mu(\mu+\delta_1+\alpha_1+\alpha_2)}, \tag{28}$$

$$R_0 = \frac{\mathrm{A}}{\mu(\mu+\delta_1+\alpha_1+\alpha_2)}[\frac{\beta_1}{N} + \frac{\beta_2\wp}{\delta_2\kappa}]. \tag{29}$$

The basic reproduction number, or R_0, measures the average number of newly infected people that are created in a population of susceptible people by a single infected person. Its value indicates the probability that an epidemic will occur [3, 21].

2.3.2 Analysis of local stability.

We are now going to look at equilibrium behavior and stability, E^0_{eq} and E^*_{eq}.

The state of DFE

This section looks at the Cholera DFE's local stability.

Theorem 2. The equilibrium $E^0_{eq} = (\frac{A}{\mu}, 0, 0)$ for the system (22) that is free of the Cholera disease is asymptotically stable when $R_0 \prec 1$ and unstable when $R_0 \succ 1$.

Proof. At E_{eq}, the Jacobian matrix is provided by

$$J(E_{eq}) \tag{30}$$
$$= \begin{pmatrix} -\mu - \beta_1 \frac{I}{N} - \beta_2 \frac{B}{\kappa + B} & -\beta_1 \frac{S}{N} & -\beta_2 \frac{S(\kappa + B) - SB}{(\kappa + B)^2} \\ \beta_1 \frac{I}{N} + \beta_2 \frac{B}{\kappa + B} & \beta_1 \frac{S}{N} - (\mu + \delta_1) - (\alpha_1 + \alpha_2) & \beta_2 \frac{S(\kappa + B) - SB}{(\kappa + B)^2} \\ 0 & \wp & -\delta_2 \end{pmatrix}.$$

For the DFE, the Jacobian matrix is provided by

$$J(E^0_{eq}) = \begin{pmatrix} -\mu & -\beta_1 \frac{\mathrm{A}}{\mu N} & -\beta_2 \frac{\mathrm{A}}{\kappa \mu} \\ 0 & \beta_1 \frac{\mathrm{A}}{\mu N} - (\mu + \delta_1) - (\alpha_1 + \alpha_2) & \beta_2 \frac{\mathrm{A}}{\kappa \mu} \\ 0 & \wp & -\delta_2 \end{pmatrix}. \tag{31}$$

This matrix's characteristic equation is $det(J(E^0_{eq}) - \lambda I_3) = 0$, where I_3 is an order three square identity matrix.
Consequently, we can observe that $J(E^0_{eq})$ has the following characteristic equations $\phi(\lambda)$:

$$\phi(\lambda) = (-\mu - \lambda)[(\beta_1 \frac{\mathrm{A}}{\mu N} - (\mu + \delta_1 + \alpha_1 + \alpha_2) - \lambda)(-\delta_2 - \lambda) - \wp \beta_2 \frac{\mathrm{A}}{\kappa \mu}]. \tag{32}$$

The characteristic equation of $J(E^0_{eq})$ has the following eigenvalues:

$$\lambda_1 = -\mu,$$

and

$$\lambda^2 - \lambda[-\delta_2 + \beta_1 \frac{\mathrm{A}}{\mu N} - (\mu + \delta_1 + \alpha_1 + \alpha_2)] - \delta_2(\beta_1 \frac{\mathrm{A}}{\mu N} - (\mu + \delta_1 + \alpha_1 + \alpha_2)) - \wp \beta_2 \frac{\mathrm{A}}{\kappa \mu} = 0. \tag{33}$$

One eigenvalue is obviously negative. The characteristic equation of the following submatrix J_1 is now (33):

$$J_1 = \begin{pmatrix} \beta_1 \frac{\mathrm{A}}{\mu N} - (\mu + \delta_1 + \alpha_1 + \alpha_2) & \beta_2 \frac{\mathrm{A}}{\kappa \mu} \\ \wp & -\delta_2 \end{pmatrix}. \tag{34}$$

If the trace of $J_1 \prec 0$ and the $det(J_1) \succ 0$, then the eigenvalues are negative. The trace is

$$\begin{aligned} tr(J_1) &= \beta_1 \frac{\mathrm{A}}{\mu N} - (\mu + \delta_1 + \alpha_1 + \alpha_2) - \delta_2 \\ &= (\mu + \delta_1 + \alpha_1 + \alpha_2)[-\beta_1 \frac{\mathrm{A}}{\mu N(\mu + \delta_1 + \alpha_1 + \alpha_2)} + 1] - \delta_2 \\ &= (\mu + \delta_1 + \alpha_1 + \alpha_2)[-1 + (R_0 - \beta_2 \frac{\mathrm{A}\wp}{\delta_2 \kappa \mu(\mu + \delta_1 + \alpha_1 + \alpha_2)})] - \delta_2. \end{aligned} \tag{35}$$

Trace of $J_1 \prec 0$ if $R_0 \prec 1$, and

$$\det(J_1) = -\delta_2 \beta_1 \frac{\mathrm{A}}{\mu N} + \delta_2(\mu + \delta_1 + \alpha_1 + \alpha_2) - \wp \beta_2 \frac{\mathrm{A}}{\kappa \mu} \succ 0. \tag{36}$$

That is,

$$\begin{aligned} &\delta_2(\mu + \delta_1 + \alpha_1 + \alpha_2)[1 - \beta_1 \frac{\mathrm{A}}{\mu N[(\mu + \delta_1) + (\alpha_1 + \alpha_2)]} \\ &- \beta_2 \frac{\mathrm{A}\wp}{\delta_2 \kappa \mu[(\mu + \delta_1) + (\alpha_1 + \alpha_2)]}] \succ 0, \end{aligned} \tag{37}$$

$$\delta_2(\mu + \delta_1 + \alpha_1 + \alpha_2)[1 - \frac{\mathrm{A}}{\mu(\mu + \delta_1 + \alpha_1 + \alpha_2)}(\frac{\beta_1}{N} + \frac{\beta_2 \wp}{\delta_2 \kappa})] \succ 0), \tag{38}$$

$$\delta_2(\mu + \delta_1 + \alpha_1 + \alpha_2)[1 - R_0] \succ 0, \tag{39}$$

$$1 - R_0 \succ 0, \tag{40}$$

if

$$1 \succ R_0. \tag{41}$$

Consequently, given that each of the characteristic equation's eigenvalues (33) possess a negative real part, it is demonstrated that E^0_{eq} has a locally asymptotically stable value. □

3 Global stability

3.1 The global stability of a cholera DFE

It is essential to show that the DFE of the model (22), as defined, is GAS in order to ensure that the eradication of cholera infection is unaffected by population sizes. We will use a concept presented in [18] to demonstrate this.

Lemma 2. [12] Let us express system (22) in the following form:

$$\begin{aligned} \frac{dX}{dt} &= N(X,Z), \\ \frac{dZ}{dt} &= M(X,Z), M(X,0) = 0. \end{aligned} \tag{42}$$

In this case, the components associated with the number of uninfected people are represented by $X \in \mathbb{R}^m$, and the components associated with the number of infected people, including latent, infectious, and so on, are represented by $Z \in \mathbb{R}^n$.

The DFE state of system (22) is denoted by $E^0_{eq} = (X^*, 0), X^* = (\frac{\mathrm{A}}{\mu})$. Furthermore, let us assume the following conditions, H_1 and H_2:

$(H_1) : \frac{dX}{dt} = N(X,0)$. Hence X^* is GAS.

$(H_2) : M(X,Z) = AZ - \widehat{M}(X,Z), \widehat{M}(X,Z) \succeq 0$ for $(X,Z) \in \Omega$.

Where Ω denotes the region where the model is biologically meaningful, the Jacobian $A = \frac{\partial M}{\partial Z}(X^*, 0)$ is an M-matrix, and the off-diagonal elements of A are nonnegative.

If $R_0 \prec 1$, then the DFE state, $E^0_{eq} = (X^*, 0)$, is globally stable.

Theorem 3. If $R_0 \prec 1$, then the DFE state of the model (22) is GAS.

Proof. All we have to do is demonstrate that when $R_0 \prec 1$, conditions (H_1) and (H_2) hold.

Given that $X = (S)$, $M = (I, B)$, and $X^* = (\frac{\mathrm{A}}{\mu})$ in our system (1), then

$$M(X,Z) = \begin{bmatrix} \beta_1 \dfrac{SI}{N} - I(\mu + \delta_1 + \alpha_1 + \alpha_2) + \beta_2 \dfrac{SB}{\kappa + B} \\ \wp I - \delta_2 B \end{bmatrix}, \tag{43}$$

and

$$A = \begin{pmatrix} \beta_1 \dfrac{\mathrm{A}}{\mu N} - (\mu + \delta_1 + \alpha_1 + \alpha_2) & \beta_1 \dfrac{\mathrm{A}}{\kappa \mu} \\ \wp & -\delta_2 \end{pmatrix}. \tag{44}$$

Undoubtedly, this is an M-matrix. Meanwhile,

$$\widehat{M}(X,Z) = \begin{pmatrix} \beta_2 \dfrac{B^2}{\kappa(\kappa + B)} S \\ 0 \end{pmatrix}. \tag{45}$$

It is clear that for $\widehat{M}(X,Z) \geq 0$, the conditions (H_1) and (H_2) have been satisfied, and as a result, E^0_{eq} is GAS since $0 \leq S \leq \frac{\mathrm{A}}{\mu}$. □

3.2 The equilibrium of the cholera disease is examined for global stability.

The following is the ultimate outcome of the global stability of $E^*_{eq} = (S^*, I^*, B^*)$ in this section.

Theorem 4. The current equilibrium point of the cholera epidemic, E^*_{eq}, is GAS if $R_0 > 1$.

Proof. When the model (22) is solved steadily, the result is

$$B^* = \frac{\wp}{\delta_2} I^*, \tag{46}$$

$$S^* = \frac{N(\delta_2\kappa + \wp I^*)(\mu + \delta_1 + \alpha_1 + \alpha_2)}{\beta_1(\delta_2\kappa + \wp I^*) + \beta_2 N \wp}. \tag{47}$$

The following results from substituting (35) and (36) into system (22)'s first equation:

$$a_1 I^{*2} + a_2 I^* + a_3 = 0, \tag{48}$$

where

$$\begin{cases} a_1 = -(\mu + \delta_2 + \alpha_1 + \alpha_2)\beta_1\wp, \\ a_2 = A\beta_2\wp - N(\mu + \delta_2 + \alpha_1 + \alpha_2)(\mu\wp + \delta_2\kappa\frac{\beta_1}{N} + \beta_2\wp), \\ a_3 = (\mu + \delta_2 + \alpha_1 + \alpha_2)\mu N\delta_2\kappa[R_0 - 1]. \end{cases} \tag{49}$$

If (48) has real, positive roots, then the system (22) is in endemic equilibrium. We apply Descartes' rule of signs to ascertain whether positive roots exist [15]. It follows that the model has a unique endemic equilibrium whenever $R_0 \succ 1$ since the sign of a_1 is negative and the sign of a_2 is positive.

□

4 Sensitivity analysis of R_0

Sensitivity analysis is an effective method for assessing how modifications to parameter values impact the robustness of a model. It assists in determining the important parameters affecting the reproduction number R_0, particularly when taking into account assumptions about parameter values and data col-

lection uncertainties. Using the methodology described in Chitnis et al. [5], we calculate the R_0 normalized forward sensitivity indices.

Let

$$\mathrm{T}_u^{R_0} = \frac{\partial R_0}{\partial u} * \frac{u}{R_0}. \tag{50}$$

Table 1 provides the sensitivity index of R_0 with respect to the parameter u.

Table 1 demonstrates that the threshold R_0 is correspondingly sensitive to

Table 1: Sensitivity indices of R_0

Parameter	Description	Sensitivity indices
A	New populations are added to the model at a constant rate.	1.0000
μ	The natural death rate	1.0000
β_1	Transmission rate from human to human	1.0000
β_2	Transmission rate from environment to human	1.0000
α_1 ; α_2	Recovery rate from cholera	-1.5504
κ	Concentration of Vibrio cholera	-1.0000
δ_1	The death rate induced by the cholera	-0.1008
δ_2	Bacteria death rate	-0.9706
$\wp$	Shedding rate of bacteria by infectious population	1.0000

variations in the parameter values A, β_1, β_2, and $\wp$. This suggests that the models will have an increase or decrease in R_0 when the values of each of the parameters in this instance increase or decrease. Conversely, the threshold R_0 is inversely proportional to the variation in μ, α_1, α_2, δ_1, and κ. In this case, a rise or fall in the values of each parameter results in an equivalent rise or fall in R_0.

5 Numerical simulations

We provide numerical solutions to model (Figure 1) for a variety of parameter values in this section. In order to solve system (1), Gumel, Shivakumar, and Sahai [9] created the Gauss-Sade-like implicit finite-difference method (GSS1 method), which is described in [12].

The fundamental data values:

The model's parameters are displayed in Table 2. The sources are also cited. First, we graphically depict the cholera DFE E_{eq}^0. Our initial values and parameters are the same as those in Table 2 $R_0 < 1$.

Using the different values of the initial variables $S(0)$, $I(0)$, $C(0)$, and $R(0)$, the following observations were obtained from these Figures 2–9. The number of possible individuals increases and gets closer to $S(0) = 250$.

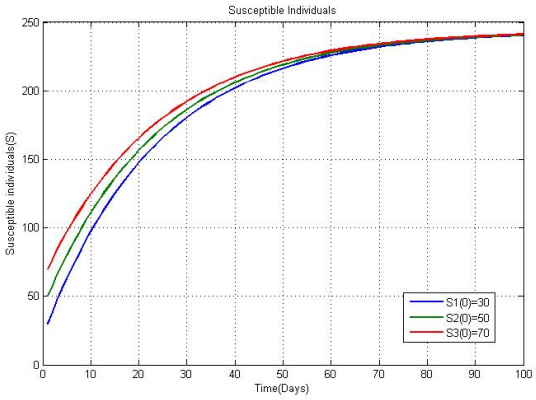

Figure 2: Susceptible individuals.

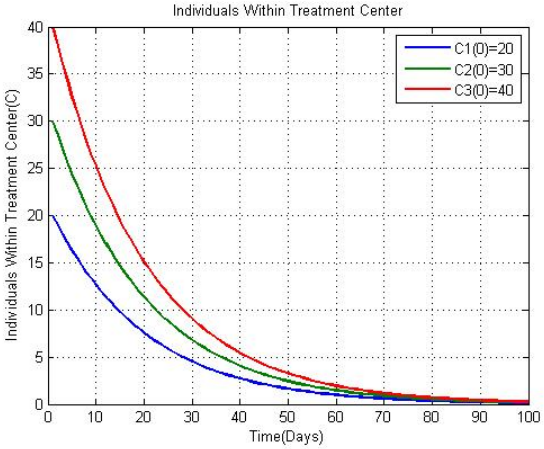

Figure 3: Individuals within treatment center.

The number of carriers and symptomatic infected individuals rises initially, then falls until it almost reaches zero.

The quantity of recovered cases declines until it almost reaches zero.

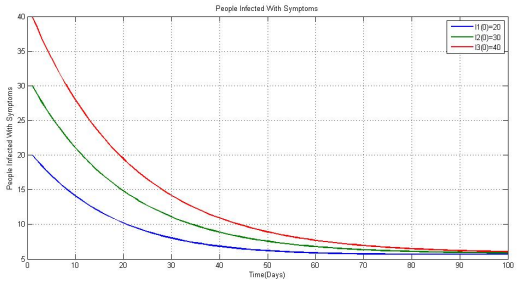

Figure 4: People Infected with symptoms.

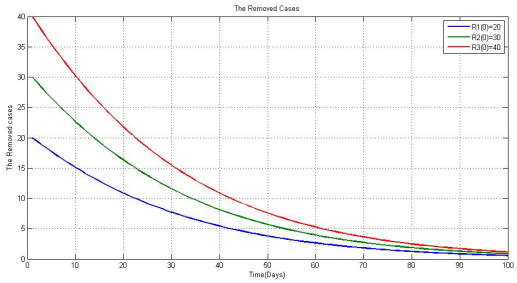

Figure 5: The Removed cases.

We possess an equilibrium for cholera disease with $R_0 > 1$. As per Theorem 3, the cholera disease equilibrium E^*_{eq} of the system (1) is GAS. Furthermore, we begin with a graphic representation of the current equilibrium of the cholera disease $E^*_e q$ and apply the same parameters and initial values in Table 2, $R_0 > 1$.

The total number of possible individuals rises initially, then somewhat declines and gets close to $S^* = 42$. The percentage of infected cases that show no symptoms or only minor symptoms initially declines quickly before slightly increasing.

The patient population at the treatment center is advancing towards the threshold of (22).

The number of carriers of the bacteria and symptomatic infected individuals converge at $I^* = 24$.

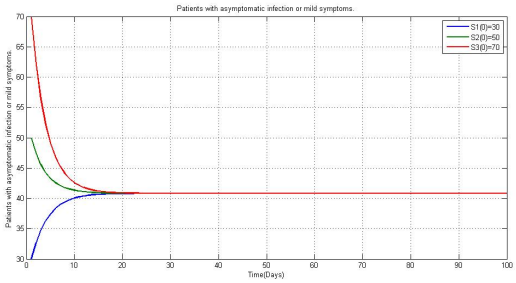

Figure 6: Patients with asymptomatic infection or mild symptoms.

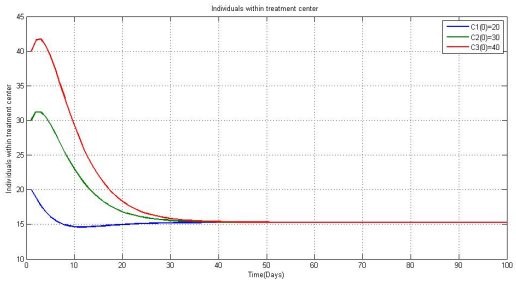

Figure 7: Individuals within treatment center.

Table 2: Baseline parameter values for system (22)

Parameter	Baseline value	Reference
A	10	Assumed
μ	0.025	[7]
β_1	0.02	[10]
β_2	0.02	[10]
α_1 ; α_2	0.214	[7]
κ	$10^4 cell/day$	Assumed
δ_1	0.013	[23]
δ_2	0.33	[14]
$\wp$	10 cell/day	[23]

Discussion of result:

A further qualitative examination of the model indicates that its solutions are both positively invariant and bound. For the study of cholera infection,

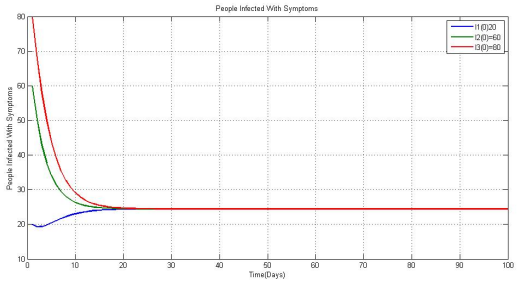

Figure 8: People Infected With Symptoms.

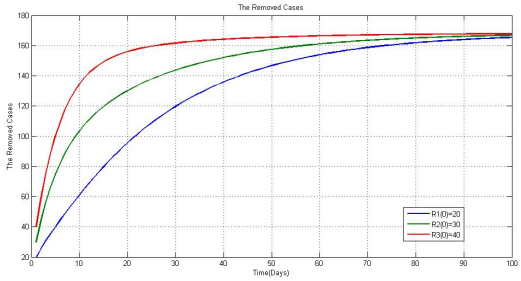

Figure 9: People Removed cases.

the basic reproduction number is required, as follows:

$$R_0 = \beta_1 \frac{\mathrm{A}}{\mu N(\mu + \delta_1 + \alpha_1 + \alpha_2)} + \beta_2 \frac{\mathrm{A}\wp}{\delta_2 \kappa \mu(\mu + \delta_1 + \alpha_1 + \alpha_2)}. \tag{51}$$

The calculation was performed utilizing the next-generation methodology, serving as a benchmark to anticipate outbreaks and evaluate control measures. The stability analysis of the DFE was also conducted employing the linearization method, with R_0 as the pivotal parameter. When the basic reproduction number is less than one, Theorem 2 and Lemma 2 indicate that the DFE is asymptotically stable both locally and globally. This means that cholera can be eliminated from the population if the initial population sizes are within the DFE's basin of attraction, E_0. Furthermore, Lemma 2 demonstrates that the DFE is GAS, implying that cholera can be eliminated regardless of the initial population size.

6 Conclusion

In this work, we formulated and presented a continuous SICR-B mathematical model of cholera disease that describes the dynamics of individuals infected with this disease. We found that

$$R_0 = \beta_1 \frac{\mathrm{A}}{\mu N(\mu + \delta_1 + \alpha_1 + \alpha_2)} + \beta_2 \frac{\mathrm{A}\wp}{\delta_2 \kappa \mu(\mu + \delta_1 + \alpha_1 + \alpha_2)}$$

is the basic reproduction number of the system, which is a crucial indicator in understanding the system's dynamics and the progression of the disease. These results help us identify the key factors influencing disease spread and control. We also performed a sensitivity analysis of the model parameters to determine which parameters have the most significant impact on the reproduction number R_0. This study highlights the importance of identifying the factors that contribute the most to the spread of the disease, thereby guiding policymakers in optimizing prevention and treatment strategies.

We applied the stability analysis theory for nonlinear systems to analyze the mathematical model of cholera and to study the local and global stability of the disease. The results show that the local asymptotic stability of the DFE E^0_{eq} can be achieved if $R_0 \leq 1$, meaning the disease will eventually die out over time. On the other hand, if $R_0 > 1$, then cholera reaches an equilibrium state E^*_{eq} and remains locally stable, indicating the persistence of the disease.

These results significantly contribute to achieving the overall objectives of the study by improving the understanding of cholera transmission dynamics and providing deeper insights into how to control the disease. Highlighting the most influential factors affecting the basic reproduction number allows for the development of more effective preventive strategies to reduce cholera spread.

Looking ahead, we aim to explore the use of fractional derivatives within a spatiotemporal framework to deepen our understanding of cholera transmission dynamics. This approach is expected to capture complex spatial and temporal patterns, thereby enhancing the accuracy of disease forecasts and control strategies.

Acknowledgements

Authors are grateful to there anonymous referees and editor for their constructive comments.

Conflicts of interest

The authors declare no conflicts of interest.

References

[1] Agarwal, R.P. *Difference equations and inequalities: Theory, methods, and applications,* CRC Press, 2000.

[2] Akinsulie, O.C., Adesola, R.O., Aliyu, V.A., Oladapo, I.P. and Hamzat, A. *Epidemiology and Transmission Dynamics of Viral Encephalitides in West Africa*. Infect Dis Rep. 2023 Sep 5;15(5):504-517. doi: 10.3390/idr15050050.

[3] Bani-Yaghoub, M., Gautam, R., Shuai, Z., Van Den Driessche, P. and Ivanek, R.*Reproduction numbers for infections with free-living pathogens growing in the environment,* J. Biol. Dyn. 6 (2) (2012) 923–940.

[4] Bouaine, A., Rachik, M. and Hattaf, K. *Optimization strategies are applied to discrete epidemic models with specific nonlinear incidence rates,* Int. J. Math. Appl. 4 (2016) 73–80.

[5] Chitnis, N., Hyman, J.M. and Cushing, J.M. *Determining important parameters in the spread of malaria through the sensitivity analysis of a mathematical model,* Bull. Math. Biol. 70 (2008) 1272–1296.

[6] Codeço, C.T. *Endemic and epidemic dynamics of cholera: The role of the aquatic reservoir,* BMC Infect. Dis. 1 (2001) 1–14.

[7] Falaye, A.J., Awonusi, F., Eseyin, O. and Eboigbe, G. *The weak form market efficiency and the Nigerian stock exchange,* Afro Asian Journal of Social Sciences, 9 (4) (2018).

[8] Ferguson, N. *Capturing human behaviour.* Nature 446, (7137) (2007) 733–733.

[9] Gumel, A.B., Shivakumar, P.N. and Sahai, B.M. *A mathematical model for the dynamics of HIV-1 during the typical course of infection,* Nonlinear Anal. Theory Methods Appl. 47 (3) (2001) 1773–1783.

[10] Hartley, T.W. *Public perception and participation in water reuse,* Desalination 187 (1-3) (2006): 115–126.

[11] Hu, Z., Teng, Z. and Jiang, H. *Stability analysis in a class of discrete SIRS epidemic models,*Nonlinear Anal. Real World Appl. 13 (5) (2012) 2017–2033.

[12] Karrakchou, J., Rachik, M. and Gourari, S. *Optimal control and infectiology: application to an HIV/AIDS model,* Appl.Math. Comput. 177 (2) (2006) 807–818.

[13] Kot, M. *Elements of mathematical ecology,* Cambridge University Press, 2001.

[14] Kumar, P., Mishra, D.K., Deshmukh, D.G., Jain, M., Zade, A.M., Ingole, K.V., Goel, A.K. and Yadava. P.K. *Vibrio cholerae O1 Ogawa El Tor strains with the ctxB7 allele driving cholera outbreaks in southwestern India in 2012,* Infect. Genet. Evol. 25 (2014) 93–96.

[15] Liu, L., Wong, Y.S. and Lee, B.H.K. *Application of the Centre Manifold Theory in Non-Linear Aeroelasticity*, Journal of Sound and Vibration. 234 (4) (2000) 641–659.

[16] Mwasa, A. and Tchuenche, J.M. *Mathematical Analysis of a Cholera Model with Public Health Interventions.* Biosystems 105 (3) (2011) 190–200.

[17] Nelson, E.J., Harris, J.B., Glenn Morris Jr, J., Calderwood, S.B. and Camilli, A. *Cholera transmission: The host, pathogen and bacteriophage dynamic,* Nat. Rev. Microbiol. 7(10) (2009) 693–702.

[18] Okolo, P.N., Magaji, A.S., Joshua, I. and Useini, P.F. *Mathematical modelling and analysis of cholera disease dynamics with control* FUDMA J. Sci. 4 (4) (2020) 363–381.

[19] Samanta, S., Rana, S., Sharma, A., Misra, A.K. and Chattopadhyay, J. *Effect of awareness programs by media on the epidemic outbreaks: A mathematical model,* Appl. Math. Comput. 219 (12) (2013) 6965–6977.

[20] Sebastian, E. and Victor, P. *Optimal control strategy of a discrete-time svir epidemic model with immigration of infectives,* Int. J. Pure Appl. Math. 113 (8) (2017) 55–63.

[21] Tahir, M., Inayat Ali Shah, S., Zaman, G. and Muhammad, S. *Ebola virus epidemic disease its modeling and stability analysis required abstain strategies,* Cogent Biol. 4 (1) (2018) 1488511.

[22] Van den Driessche, P. and Watmough, J. *Reproduction numbers and sub-threshold endemic equilibria for compartmental models of disease transmission,* Math. Biosci. 180 (1-2) (2002) 29–48.

[23] Vashist, A., Verma, J., Narendrakumar, L. and Das, B. *Molecular Insights into Genomic Islands and Evolution of Vibrio cholerae,* In Microbial Genomic Islands in Adaptation and Pathogenicity: Springer, 2023.

[24] Wang, J. and Modnak, C. *Modeling cholera dynamics with controls,* Can. Appl. Math. Q. 19 (3) (2011) 255–273.

[25] Watson, A.P., Armstrong, A.Q., White, G.H. and Thran, B.H. *Health-based ingestion exposure guidelines for Vibrio cholerae: Technical basis for water reuse applications,* Sci. Total Environ. 613 (2018) 379–387.